12-T

TEMPERATURE MEASUREMENTS IN WIND TUNNELS BY ELECTRONIC PHASE-SHIFT METHODS

A THESIS

Presented to

the Faculty of the Graduate Division

by

Theodore Jay Gordon

In Partial Fulfillment

of the Requirements for the Degree

Master of Science in Aeronautical Engineering

Georgia Institute of Technology

December 1951

243341

TEMPERATURE MEASUREMENTS IN WIND TUNNELS BY ELECTRONIC PHASE-SHIFT METHODS

Approved:

[redacted]

Date Approved by Chairman: 14 Dec, 1957

ACKNOWLEDGEMENTS

The cooperation and helpful suggestions extended by Dr.Richard Fledderman, who served in the dual capacity of Committee Chairman and Thesis Advisor, are greatly appreciated by the author. The author is also particularly indebted to M.A. Honnell for his many enlightening suggestions about the electrical circuitry involved in the performance of the experiments in this Thesis. Thanks are also extended to H. S. La Vier who was kind enough to serve on the Reading Committee.

TABLE OF CONTENTS

LIST OF SYMBOLS USED IN THIS REPORT

a = Actual speed of sound

a_o = γRT

b = Damping coefficient

C_p = Specific heat at constant pressure

C_v = Specific heat at constant volume

K_2, K_3 = Constants

L = Wave length

L' = Mean free path

N = Newtonian velocity of sound -- isothermal

p = Hydrostatic pressure

p_{xx} = xx component of stress tensor

q_x = x component of heat flux vector

RN = Reynold's number

R = Universal Gas constant

r_a = Amplitude ratio

s = Condensation coordinate

t = Time

T = Absolute temperature

U = Velocity of fluid particle

V = Velocity of fluid stream

v = Volume

$\overline{\Psi}$ = Root mean square velocity

x = Distance in direction of propagation

Z' = Thermometric conductivity

α = a/a_o

β = Reciprocal of Prandtl Number $\lambda' / 4 C_p$

β' = specific heat / mol.

γ = C_p/C_v

ε = Molecular constant

θ' = Collison rate

θ_3, θ_4 = Constants

η = Molecular velocity component

λ = Bulk modulus

λ' = Coefficient of thermal conductivity

μ = Coefficient of absolute viscosity

ρ = Density

σ = Imposed frequency

ν = Frequency in cycles per second

ϕ = Phase shift

$( )_o$ = Undisturbed value

$( )'$ = Perturbation value of variable

$( )^*$ = Dimensionless form of variable

LIST OF TABLES

LIST OF FIGURES

TEMPERATURE MEASUREMENT IN WIND TUNNELS BY ELECTRONIC PHASE-SHIFT METHODS

SUMMARY

The object of this thesis is to develop theoretical methods of measuring temperature changes by phase-shift observations, to verify these theoretical approaches by experiments, and to apply these methods to the measurement of the temperature of the air stream of a subsonic and a supersonic wind tunnel.

A review of pertinent literature is first conducted in order to determine the relative importance of the various parameters affecting the velocity of propagation of sound. Knowing the effect of these parameters in the present applications, two general relationships are derived which related changes in phase to changes in temperature. These relationships are verified in laboratory experiments and then applied to the measurement of temperature in a subsonic and a supersonic wind tunnel.

In both cases the phase-shift methods give good results. In the supersonic application, the methods show considerable promise and are worthy of further development. For precise temperature measurement in the supersonic wind tunnel, the temperature field would have to be uniform. Nonuniformity is introduced because of the temperature gradient in the boundary layer. Further refinement of the methodology could conceivably produce an instrument for use in boundary layer analysis.

CHAPTER I

INTRODUCTION

The measurement of temperature of moving streams of air by ordinary thermometric means usually posseses two intrinsic disadvantages. First, complete temperature recovery is seldom achieved in practice. Theoretically, when moving air is brought to rest in the temperature sensitive element of a moving air thermometer, its temperature will rise to the so-called "stagnation temperature" associated with the flow field. However, heat transfer and radiation within the thermometer and heat dissipation in the gas stream make this rise somewhat less than the theoretically predicted rise, and consequently, a temperature recovery factor must be introduced into the calibration of the thermometer. The temperature recovery factor is defined[1] as

$$\theta = \frac{T_w - T}{T_o - T} \tag{1}$$

where T is the static temperature of the moving stream, T_o is the stagnation temperature of the stream, and T_w is the temperature of the insulated wall. Only in the case of complete temperature recovery is the temperature at the wall equal to the stagnation temperature, and in this case $\theta = 1$.

The methods which are derived in this paper are independent of temperature recovery factor considerations and measure directly the mean static temperature of the moving stream. However, only in the case of a homogeneous, uniform stream is this temperature exactly equal to T in the above equation.

A second intrinsic disadvantage associated with a moving air thermometer is the fact that by virtue of its insertion into the stream, the characteristics of flow of the stream will change. The temperature measurement is generally not simultaneous with the model testing for this reason.

Two electronic, phase-shift methods for measuring temperature of moving streams are developed in this thesis. The methods have the advantages of being independent of temperature recovery factor considerations, and of eliminating the necessity for disturbing the mass of air whose temperature is being measured.

In application of this technique, a sound wave is sent across a stream of air. The wave shape of the input signal to the speaker is compared with the received wave after it has crossed the medium. In a series of consecutive comparisions, changes in the phase angle between these waves is shown to be indicative of changes in temperature of the medium. In this paper, the term "phase angle" refers to the angle between the transmitted and received wave, and the term "phase difference" refers to the changes in phase angle between two given runs.

The general phase-shift method for measuring temperature may be outlined as follows: if the distance between a sound source and sound receiver is adjusted so that at any instant, using sound at some constant frequency, there is an integral number of wave lengths between the two, then the received sound will be exactly in phase with the transmitted wave. This means that the alternating-current produced by the receiver picking up the sound pulses has amplitude peaks occurring at exactly the same time as the audio-frequency alternating-current input to the transmitting speaker. We may represent this alternating-current input to the transmitting speaker as

$$y = A \sin x \qquad (2)$$

Similarly, the alternating-current produced by the receiver picking up the sound impulses may be represented by

$$y = A_1 \sin (x + \theta) \tag{3}$$

When the phase angle θ, is zero, the transmitted and received waves are in phase.

It is obvious that the number of waves which exist between the sound transmitter and receiver is dependent on the speed of sound, the frequency of the sound being transmitted, and the distance between the transmitting and receiving units. This is true since

$$L = \frac{a}{v} \tag{4}$$

Changes in the speed of sound (for fixed frequency and distance) can be observed by noting changes in wave length or total number of waves. This change in the total number of waves puts the transmitted wave and the received wave out of phase. By noting the amount of phase difference, the change in the speed of sound can be derived, and from the classical relationship

$$a_o = (\gamma RT)^{\frac{1}{2}} \tag{5}$$

the changes in temperature can be found.

However, before this relationship between the speed of sound and temperature may be used, its adequateness must be investigated. It is derived on the basis of the assumption that frequency, viscosity, and heat transfer effects can be ignored. Whether these assumptions are sufficiently correct for the applications in this thesis is investigated in Chapter 2 by reviewing pertinent literature.

Hence this paper is divided into three distinct sections:

1. Review of the Literature. — Theoretical investigations into the relationship between the speed of sound and other parameters of the wave and medium.

2. Verification of experimental methods which are used in actual temperature measurement.

3. Application to the methods of temperature measurement in a supersonic wind tunnel.

CHAPTER II

REVIEW OF THE LITERATURE

A search of the literature is here conducted so that a relationship between the speed of sound, temperature, viscosity, heat conduction, relaxation time, and dispersion of the sound can be found. It is necessary to investigate these relationships first since any phase-shift, temperature method is necessarily based on it.

The simplest approximation to the problem is the familiar

$$a_o = (\gamma RT)^{\frac{1}{2}} \tag{6}$$

A derivation of this equation is made by A.Y.Pope.[2] It is derived on the assumptions that the fluid is inviscid and isentropic and that the frequency of the sound being propagated is zero. This last assumption is merely implied in the derivation.

This equation may be derived by considering the sound wave to be an infinitesimal shock wave.[3] If the conditions on the upstream side of the wave are ρ, u, p and those downstream of the wave are $\rho+\Delta\rho$, $p+\Delta p$, $u+\Delta u$, the equations of continuity and momentum may be written as

$$\rho u = (\rho + \Delta\rho)(u + \Delta u) \tag{7}$$

$$p - (p + \Delta p) = (\rho + \Delta\rho)(u + \Delta u)^2 - \rho u^2 \tag{8}$$

Then on expanding Eq. (7) and dividing it by Eq. (6) the following relationship is obtained.

$$u^2 = \frac{-\Delta p - \Delta u(u\Delta\rho + \rho\Delta u + \Delta u\Delta\rho)}{\Delta\rho - \Delta\rho\frac{\Delta u}{u}} \tag{9}$$

Then if the discontinuity, Δu, is very small

$$a = \sqrt{\frac{dp}{d\rho}} \tag{10}$$

Horace Lamb[4] proves by methods of kinematics and fluid dynamics that the speed of sound, to a first approximation, is independent of heat conduction and viscosity. He first considers the case of viscosity alone. The Navier-Stokes equation expressing the motion of the fluid in the x direction is

$$\frac{\partial u}{\partial t} = -\frac{1}{\rho_0}\frac{\partial p}{\partial x} + \frac{4}{3}\frac{\mu}{\rho}\frac{\partial^2 u}{\partial x^2} \tag{11}$$

A condensation parameter S is defined as follows

$$\frac{\partial s}{\partial t} = -\frac{\partial u}{\partial x} \tag{12}$$

The physical thermodynamic equation for the medium is

$$p = \rho_0 + a_0^2 \rho_0 s \tag{13}$$

If p and S are eliminated between Eq. (11) and (13), Eq. (14) is obtained

$$\frac{\partial^2 v}{\partial t^2} = a_0^2 \frac{\partial^2 v}{\partial x^2} + \frac{4}{3}\frac{\mu}{\rho}\frac{\partial^2 v}{\partial x^2} \tag{14}$$

The vibration

$$v = a e^{i\sigma t} \tag{15}$$

is imposed on the medium at a point in the fluid where x 0; σ being the imposed frequency in radians/sec, A solution of the form

$$v = A_1 e^{i\sigma t + mx} \tag{16}$$

is assumed for Eq. (14). By substituting this solution back into Eq.(14) it is found that

$$-\sigma^2 = m^2 \left(a_0^2 + \frac{4}{3} i \frac{\mu}{\rho} \sigma\right) \tag{17}$$

If Eq. (17) is solved for m, Eq. (18) is obtained.

$$m = \pm \frac{i\sigma}{a_0} \left(1 - \frac{4}{3} i \frac{\mu}{\rho} \frac{\sigma}{a_0^2}\right)^{-\frac{1}{2}} \tag{18}$$

If the $\left(1 - \frac{4}{3} \frac{\mu}{\rho} \frac{\sigma}{a_0^2}\right)^{-\frac{1}{2}}$ term is expanded into an infinite series and the square terms of $\frac{\mu}{\rho} \frac{\sigma}{a_0^2}$ are neglected and the lower sign is chosen, then

$$m = -\frac{i\sigma}{a_0} - \frac{2}{3} \frac{\mu}{\rho} \frac{\sigma^2}{a_0^3} \tag{19}$$

Upon replacing this value of m in the assumed solution it is seen that

$$v = a_0 e^{i\sigma t - \left(-\frac{i\sigma}{a_0} + \frac{2}{3} \frac{\mu}{\rho} \frac{\sigma^2}{a_0^3}\right) x} \tag{20}$$

or

$$v = a_0 e^{-x\left(\frac{2}{3} \frac{\mu}{\rho} \frac{\sigma^2}{a_0^3}\right)} e^{i\sigma t - \frac{i\sigma x}{a_0}}$$

$$= a_0 e^{-x\left(\frac{2}{3} \frac{\mu}{\rho} \frac{\sigma^2}{a_0^3}\right)} e^{i\sigma\left(t - \frac{x}{a_0}\right)}$$

$$= a_0 e^{-x/\ell} \cos \sigma \left(t - \frac{x}{a_0}\right) \tag{21}$$

where $\ell = \frac{3}{2} \frac{\rho}{\mu} \frac{a_0^3}{\sigma^2}$. This equation describes the oscillatory motion of a particle within the fluid as a wave passes over it. Since the exponent of e describes the amplitude of the wave, it can be seen that the amplitude decreases as the x distance increases and the rate of decrease is

greater for higher values of frequency σ. Since the frequency of the wave is unaffected by distance, it may be concluded that the speed of the wave is unaffected by friction, at least for first power terms of $\frac{\mu}{\rho}\frac{\sigma}{a_0^2}$ because higher degree terms were omitted when expanding Eq. (15).

Lamb reaches a similar conclusion when he considers the effects of heat conduction as well as viscosity. Therefore he concludes that neither viscosity nor heat conduction, to a first approximation for ordinary audio-frequencies, affects the wave propagation velocity.

Tsien and Schamberg[5], seeking a more exact proof, use the second-order approximations to the Navier-Stokes and energy equations. Lamb uses these equations in the following form.

Navier-Stokes: (22)

$$\frac{\partial v}{\partial t} = -\frac{1}{\rho_0}\frac{\partial p}{\partial x} + \frac{4}{3}\frac{\mu}{\rho}\frac{\partial^2 v}{\partial x^2}$$

Energy: (23)

$$\frac{\partial T}{\partial t} = \frac{\lambda'}{\rho_0 C_v}\frac{\partial^2 T}{\partial x^2} - (\gamma-1)\frac{T_0}{v_0}\frac{\partial v}{\partial t}$$

By the kinetic theory of gases, it may be shown that the viscous stresses in the Navier-Stokes equation and the heat flux terms of the energy equation are only first-order approximations which become different from reality if the density of the gas is low or if the wave length of the sound is small. Tsien and Schamberg's derivation makes use of the second-order approximation to these equations developed by Chapman and Cowling.[6] These equations may be compared with Eq. (22) and (23) above.

Navier-Stokes: (24)

$$\frac{\partial v'}{\partial t'} = -\frac{1}{\rho_0}\frac{\partial p'}{\partial x} + \frac{4}{3}\frac{\mu}{\rho}\frac{\partial^2 v}{\partial x^2} + \frac{2}{3}\frac{\mu^2}{\rho}\left(\frac{\kappa_2}{\rho_0\rho_0}\frac{\partial^3 \rho'}{\partial x^3} - \frac{\kappa_3}{\rho_0 T_0}\frac{\partial^3 T'}{\partial x^3}\right)$$

Energy: (25)

$$\frac{\partial T'}{\partial t} = \frac{1}{\rho_0 C_p}\left\{\frac{\partial p'}{\partial t} + \lambda'\frac{\partial^2 T'}{\partial x^2} - \frac{2}{3}(\theta_2+\theta_4)\frac{\mu^2}{\rho_0}\frac{\partial^3 v'}{\partial x^3}\right\}$$

where K_2, K_3, θ_2, θ_4 are constants depending on the molecular structure of the gas.

Tsien and Schamberg define a deviation factor $\alpha = a/a_o$, where a is the actual speed of sound and a_o is the adiabatic speed of sound. The solution for α appears in the form of an infinite series.

$$\alpha = 1 + \frac{.7807}{RN^2} - \frac{4.2314}{RN^4} - \frac{2.8344}{RN^6} \qquad (26)$$

where R.N. is defined as $\frac{\rho a_o L}{2\pi\mu}$. The constants in the above equation represent the solution for air at atmospheric pressure.

The deviation dispersion factor α, was plotted against R.N. in Fig. 10. This plot shows the variation of the correctness of the adiabatic speed of sound assumption with the wave length of the propagated sound and the density. It may be noted that the greatest deviation is obtained at low R.N.; i.e. at low wave lengths or low densities. Since R.N. $= \frac{\rho a_o L}{2\pi\mu}$ and $\alpha = a/a_o$ it is seen that as the density decreases, or the wave length becomes smaller, the R.M. decreases and the actual speed of sound, a, diverges further from the isentropic speed of sound, a_o. Since ρ and L both appear to the first power in the numerator of the R.M. expression, to produce a given change in α, either ρ or L may be changed by the same percentage. Doubling the frequency would have the same effect on α as would decreasing the density by one half. This immediately suggests that the effects of high altitudes on sould propagation may be studied expediently by controlling the frequency of the sound on which the experiments are being conducted.

In a report published at the University of Michigan[7], C.S. Wang Chang and G.E. Ulenbeck point out that the Chapman and Cowling derivation

of the second-order Navier-Stokes equation is in error, and consequently the work of Tsien and Schamberg based on Chapman's derivation is in error. Chang, in a later report,[8] finds that when using Burnett's molecular approximations to the Navier-Stokes equation

$$a = a_0 \left\{ 1 + \left(\frac{2}{3} + \frac{5}{9}\epsilon_3\right)\frac{\mu^2\omega^2}{\rho_0^2 a_0^4} + \left(\frac{5}{3} - \frac{4}{9}\epsilon_2\right)\frac{\mu\nu'\omega^2}{\rho_0^2 a_0^4} - \frac{\nu'^2\omega^2}{\rho_0^2 a_0^4}\left(\frac{3}{8} + \frac{2}{9}\epsilon_1\right) \right\} \qquad (27)$$

where: ϵ_{123} = are molecular constants

ω = angular frequency of sound

ν' = is defined by $\nu' = s\mu$

s = a dimensionless temperature dependent quantity

Applying this relationship to helium, Chang finds

$$\alpha = 44.4\mu^2\left(\frac{\nu}{p}\right)^2 \qquad (28)$$

where μ is in c.g.s. units, ν in megacycles per second, and p is in atmospheres. Thus for very high frequencies or for very low pressures, the isentropic assumption is no longer valid. However, in the range of audio frequencies and normal temperatures and pressures, the assumption that

$$a = a_0 = (\gamma RT)^{\frac{1}{2}} \qquad (29)$$

is quite adequate as $\alpha \approx 0$ from 13.

In polyatomic gases there is an additional dispersion of the sound caused by the internal degrees of freedom of the molecules. The relaxation time, τ, is a measure of the relative ease with which the internal motion of the molecules in the medium conducting the sound comes

to equilibrium with the translational motion. If we accept the possibility of an exchange of energy between the translational and internal degrees of freedom, the Stokes relationship

$$2\mu + 3\lambda = 0 \tag{30}$$

is no longer valid and a coefficient K may be defined by

$$K = \lambda + \frac{2}{3}\mu \tag{31}$$

K is known as the Tisza coefficient. It gives the second-order correction [10] to the hydrostatic pressure arising from compression or expansion.

$$p = p_0 + K\left(\frac{1}{\rho}\right)\frac{d\rho}{dt} \tag{32}$$

The pressure in a fluid depends not only on the instantaneous value of the density and temperature, but also on the rate of change of the density of the fluid. Therefore in problems where frequencies are very high or densities are very low, Eq. (19) should be introduced into the Navier-Stokes equation.

The relaxation time is related to by

$$\tau = \frac{3}{2}\eta\frac{C_v^2}{\beta^2\gamma T}K \tag{33}$$

where β is the specific heat per molecule due to internal motion and η is the molecular velocity component. For the case of no internal degrees of freedom, K vanishes and τ goes to 0.

Physically, if θ' is the collision rate of molecules in a gas

$$\tau = \frac{1}{\theta'} \tag{34}$$

Then, by considering a Maxwellian distribution of the molecular velocities, τ is the time it would take for $1 - 1/L'$ molecules to collide, where L' is the mean free path of the molecules. If $\bar{V}$ is the root-mean-square velocity of the molecules

$$\theta' = \frac{\bar{V}}{L'} \tag{35}$$

and

$$\tau = \frac{L'}{\bar{V}} \tag{36}$$

In most cases τ is very short and may be neglected so that κ is zero. However, if the pressure is very low, L' is large, τ becomes large and κ is appreciable. Experiments indicate that the rotational relaxation time for diatomic gases under atmospheric pressure is of the order of 10^{-8} to 10^{-9} seconds.[11] The assumption that

$$2\mu + 3\lambda = 0 \tag{37}$$

is justified if and only if[12]

$$\nu \ll \tau^{-1} \tag{38}$$

CHAPTER III

DEVELOPMENT OF PHASE-SHIFT EQUATIONS

PHASE-ANGLE OBSERVATION METHOD.— It was shown previously in this paper that if the distance between a sound and receiver is adjusted so that an integral number of wave lengths exist between them, there is zero phase shift between the transmitted and the received wave.

If these waves are superimposed on the horizontal and vertical axes of a single oscilloscope, a pattern known as a Lissajous figure is obtained. This pattern is shown in Fig. 1 for the case of in-phase waves.

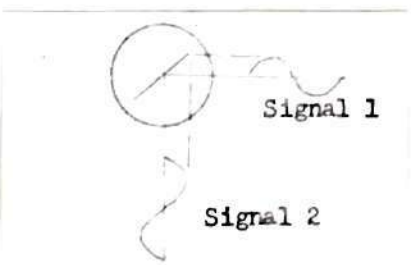

Figure 1
In-Phase Lissajous Pattern

If the temperature of the medium conducting the sound is increased, the speed of the sound wave moving through it will increase. As a result, there will be fewer waves between the units if the frequency is kept constant since

$$a = v_L \tag{39}$$

When these waves are superimposed on an oscilloscope, the Lissajous figure changes from a straight line to a circle or ellipse, since, in general, these waves will be out of phase. This trace is shown in Fig. 2.

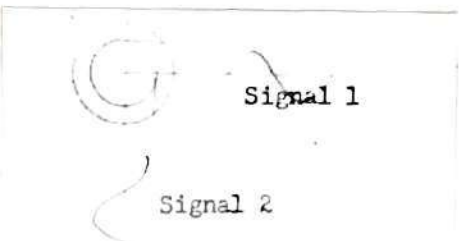

Figure 2
Out-of-Phase Lissajous Pattern

Thus a phase shift is produced by changing the temperature of the sound conducting medium. The relationship between the phase shift and the temperature must be investigated.

In the review of the literature it was shown that transmitted sound waves whose frequencies are less than the order of magnitude of megacycles are not affected appreciably by heat dissipation, viscosity, or dispersion. Therefore, at audible frequencies

$$a = a_o \tag{40}$$

If the distance between the sound transmitter and receiver is x, then the number of waves, N, between them is

$$N = \frac{x}{\lambda} = \frac{x\nu}{a_o} = \frac{x\nu}{\sqrt{\gamma RT}} \tag{41}$$

When it is assumed that the phase angle is not zero, it is seen that

$$N = n_1 + N_o \tag{42}$$

where N_o is an integral number of waves and n_1 is the fractional part. Then the phase angle between the two waves is $360n_1^{\circ}$. Substituting this into Eq. (42), it is seen that

$$N_o + n_1 = \frac{x v}{\sqrt{\gamma R T}} \tag{43}$$

or

$$360\ (N_o + n_1) = \frac{360\, x v}{\sqrt{\gamma R T}} \tag{44}$$

Representing the phase angle, $360\ n_1$, by ϕ, Eq. (44) reduces to

$$360\ N_o + \phi_1 = \frac{360\, x v}{\sqrt{\gamma R T_1}} \tag{45}$$

If the temperature is changed to some new value, Eq. (45) may be written

$$360\ N_o + \phi_2 = \frac{360\, x v}{\sqrt{\gamma R T_2}} \tag{46}$$

Subtracting Eq. (46) from (45), the phase shift, $\phi_1 - \phi_2$ is obtained.

$$\phi_1 - \phi_2 = \frac{360\, x v}{\sqrt{\gamma R}} \left\{ \frac{1}{\sqrt{T_1}} - \frac{1}{\sqrt{T_2}} \right\} \tag{47}$$

Solving Eq. (47) for $(T_2)^{\frac{1}{2}}$ one obtains

$$\sqrt{T_2} = \frac{360\, x v \sqrt{T_1}}{360\, x v - \sqrt{\gamma R T_1}\ (\phi_1 - \phi_2)} \tag{48}$$

By using this method of approach, the temperature of the sound conducting medium may be determined; the only requirement is that the phase angle at some standard temperature is known.

FREQUENCY FOR ZERO PHASE-SHIFT METHOD.— A second, somewhat more simplified approach may be made to the problem. As before

$$N_o + n_1 = \frac{x \ \nu_1}{\sqrt{\gamma R} \ \sqrt{T_1}} \tag{49}$$

and

$$N_o + n_2 = \frac{x \ \nu_2}{\sqrt{\gamma R} \ \sqrt{T_2}} \tag{50}$$

In the previous derivation, the frequency was considered constant and $(n_1 - n_2)360$ was the quantity used to measure change of temperature. Now the frequency shall be considered an independent variable which can be adjusted in order to make phase angle at each new condition of temperature zero. Subtracting Eq. (50) from Eq. (49) as before, Eq. (51) is obtained.

$$n_1 - n_2 = \frac{x}{\sqrt{\gamma R}} \left\{ \frac{\nu_1}{\sqrt{T_1}} - \frac{\nu_2}{\sqrt{T_2}} \right\} = 0 \tag{51}$$

Simplifying, Eq. (51) becomes

$$\frac{\nu_1}{\sqrt{T_1}} = \frac{\nu_2}{\sqrt{T_2}} \tag{52}$$

When applying this second method, the frequency for zero phase angle at a known temperature would have to be observed first. To determine some new temperature, only the frequency which would produce zero phase angle under the new condition would have to be found.

CHAPTER IV

EXPERIMENTAL CALIBRATION

In ADIABATIC BOX.— The frequency for zero phase-shift method was first used in an actual verification experiment. Fig. 3 shows the general circuit used in the experiment.

Figure 3
Circuit in Adiabatic Box

The frequency of the audio oscillator could be varied so that the transmitted and received waves were in phase. The vacuum tube voltmeter was used in order to maintain the output of the audio oscillator at a constant level at all frequencies.

A device was constructed which would house the speaker and receiver and their associated mountings. Standard permanent magnet type earphones were used for both the speaker and sound pickup. The method of mounting these units is shown in Fig. 17 in the Appendix. The box was made of plywood and is also shown in Fig.17. The requirements which the housing had to satisfy were these: first, the temperature of the air in the box had to be variable, and as constant as possible. Second, the temperature of

the air in the box had to be observable so that the predicted temperatures could be checked. Third, the box had to be designed to have good sound absorbing qualities so that no standing waves would be reflected from the walls of the box and interfere with the phase angle observations. Fourth, the heat transfer between the box and outside air had to be kept to a minimum. Fifth, the intercapacitive coupling between the transmitting and receiving circuits had to be a minimum.

The first of these requirements, varying the temperature, was satisfied by letting a hot air blower circulate hot air into the box. The blower is shown in Fig. 18. It was found that in order to reach a condition of thermal equilibrium in the box, a Variac variable transformer had to be inserted into the 110 volt alternating-current line in series with the blower-heater. The temperature of the air in the box was observed by means of a mercurial thermometer which was placed through the wall of the box. The temperature bulb was close to, but not between, the earphones.

F.G. Tyzzer and W.C.Hardy[13] point out that felt is an effective vibration absorber and isolator for frequencies in the audible range. To satisfy condition three, then, the box was lined with soft, half-inch thick industrial packing felt. During the performance of the experiment, it was felt that some reflected waves might be producing erroneous data, so the box was completely filled with soft raw cotton (except for a channel between the phones). However, it was found that this was unnecessary and the felt was producing sufficient absorption.

Aluminum foil was placed between the felt lining and the inner wall of the box to minimize heat transfer. The foil produced adequate insulation.

Capacitive coupling was tested for by covering the receiving earphone while the transmitting earphone was operating. The major portion of any indicated output would then be caused by stray capacitive coupling. Bonding the aluminum foil lining to the receiver mountings and physically separating the input and output circuit lead-in wires, the capacitive pick-up was effectively reduced.

A cut-away sketch of the box is shown in Fig.4

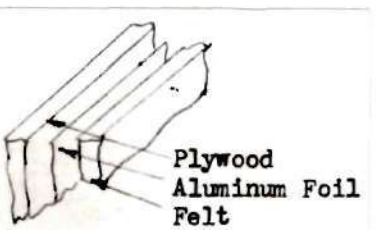

Figure 4
Box Wall

The mountings for the receivers were constructed so that the distance between the earphones was variable. The faces of the earphones were parallel at all times.

The signal generator was a Hewlett Packard Audio Oscillator. Its gain was raised so that the Lissajous pattern on the oscilloscope appeared as two parallel lines. The in-phase condition was achieved by adjusting the frequency of the oscillator, and was indicated on the oscilloscope by a coinciding of the lines forming the sides of the ellipse. Figs. 9 and 10 show the in-phase and out-of-phase conditions.

The vacuum tube voltmeter was included in the circuit so the output of the oscillator could be adjusted to the same intensity at each frequency setting. Then for various temperatures, as indicated by the mercurial thermometer in the box, the frequency for zero phase-shift was

noted. This data is shown in Table 1. Upon analyzing the data it was found that the quantity $\frac{\nu}{\sqrt{T}}$ was a constant as previously predicted in Eq. (52). The data is plotted in Fig.11.

The experiment could have been further refined by using some other type of thermometer, perhaps a thermocouple or low range mercurial thermometer. Also some sort of thermostat could be used to insure thermal equilibrium in the box. The greatest source of inaccuracy in this experiment however, was the inability to read the frequency of the audio oscillator closely enough. Therefore, some sort of crystal calibrating device could be used for more accurate determination of the audio frequency in future experiments.

The error which might be expected in the term $\frac{\nu}{\sqrt{T}}$ is now investigated. Eq. (52) may be written from Eq. (52),

$$\frac{\nu \pm d\nu}{\sqrt{T \pm dT}} = A \pm dA \tag{53}$$

where A is some constant determined by the physical characteristics of the experiment, dA is the error involved in the determination of that constant, d is the error involved in determining the frequency, and dT is the error involved in finding the temperature. It is seen that the error, dA, is a function of d ν and dT. Writing

$$A = \frac{\nu}{\sqrt{T}} \tag{54}$$

and placing in total derivative form, Eq. (55) is obtained.

$$dA = \frac{\partial}{\partial \nu}\left(\frac{\nu}{\sqrt{T}}\right) d\nu + \frac{\partial}{\partial T}\left(\frac{\nu}{\sqrt{T}}\right) dT \tag{55}$$

Taking the derivatives

$$dA = \frac{1}{\sqrt{T}}\, d\nu - \frac{1}{2}\,\frac{\nu}{T^{3/2}}\, dT \tag{56}$$

on the audio oscillator, the frequency could be read to 50 cycles in the range used and the temperature could be read to the nearest quarter of a degree. The temperatures were in the range of 300 degrees Centigrade and the frequencies were all about 4000 cycles per second. On this basis the expected error was computed.

$$dA = \pm\,\frac{25}{300^{1/2}} \pm \frac{1}{2}\,\frac{4000\,(.25)}{\sqrt{27}}\times 10^{-3} = 1.539 \tag{57}$$

The per cent accuracy which may be expected in the experiments is then

$$1 - \frac{dA}{\nu/\sqrt{T}} = 1 - \frac{1.539}{4000/\sqrt{300}} = 99.3\ \% \tag{58}$$

As seen in Fig. 11, the experimental data is well within this limit.

A second experimental method was pursued wherein the phase-shift was applied directly. The experiment was designed to make use of Eq. (48). A variety of methods have been used previously to observe phase angles directly. As in the experiment above, Lissajous figures on oscilloscope faces may be observed and the phase angle computed by noting the eccentricity of the elliptical trace. An electronic switch may be used to switch the input to the oscilloscope between the signals to be compared so that the trace on the scope is the two superimposed images. A third method using an oscilloscope has been developed by K.S. Lion.[14] Here use is made of a circular trace derived from one of the two input signals. The circular sweep is of small diameter and is expanded momen-

tarily by each of the two signals being compared, the geometrical angle between the pips being the unknown phase angle.

In addition to these oscilloscope methods, a direct reading phase angle meter has been developed by the Technology Instrument Corporation. This meter is shown in Fig. 21. It was used in measuring the phase angle needed in applying Eq. (48).

The following information is taken from the instruction manual which accompanied the Technology Instrument Corporation 320A Direct Reading Phase Meter:

> The operation of the phase meter is based on pulse methods. The two signals being compared are converted into a series of pulses. The time displacement between the pulse trains is indicative of the unknown pulse angle. The pulse trains are fed into a flip-flop circuit which measures the ratio of time displacement to the pulse repetition rate. For a given phase difference, this ratio is independent of frequency.

The method of hooking up the circuit employing the phase shift meter is shown below in Fig. 5.

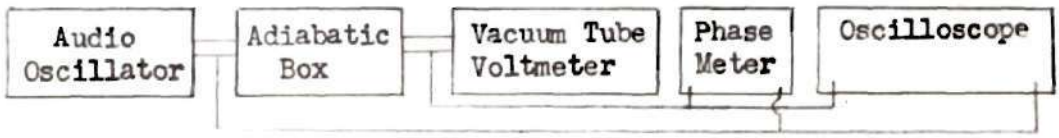

Figure 5
Phase Meter-Adiabatic Box Circuit

The oscilloscope was included in the circuit to give a visual indication of phase angle as the experiment progressed.

The phase angle for various temperatures in the box was recorded. The temperature in the box was varied by changing the setting of transformer which was in series with the blower-heater combination. A series of graphs were prepared beforehand which, for a given initial temperature,

predicted the new temperature for any observed phase shift. This data is given in Table 2 and is plotted in Fig. 14. The experiment was performed using different initial temperatures. The experimental data are presented in Table 3 and are superimposed on the theoretical phase shifts in Fig. 12.

There were two general difficulties encountered in the performance of this experiment. First, hum modulation originating in the stray pick-up of the connecting wires caused an erroneous indication of phase angle. The use of shorter, shielded leads corrected this difficulty. Also, the phase shift meter was very sensitive to the rapid temperature fluctuations arising in the blower. An accurate, stabilized reading was difficult to obtain under these conditions. This situation was corrected by filling the box with absorbent cotton, except for a channel between the phones, to reduce the effect of direct blast between the phones.

The probable error which may be encountered in using this method may be computed. Since in any given set of data, the quantities of frequency, distance between phones, and initial temperature may be considered constant, Eq. (48) may be written in the following form.

$$\sqrt{T_2} = \frac{K}{C - D\Delta\phi} \tag{59}$$

Where:

$$K = 360 \times \nu \sqrt{T_1} \tag{60}$$

$$C = \frac{K}{\sqrt{T_1}} = 360 \times \nu$$

$$D = \sqrt{\gamma R T_1} = a_0,$$

By simplifying and differentiating Eq. (59), Eq. (61) is obtained.

$$\frac{1}{\sqrt{T_2}}\left\{\frac{C}{2} - \frac{D}{2}\Delta\phi\right\} dT_2 = D\sqrt{T_2}\, d\Delta\phi \qquad (61)$$

If values which result from taking the initial temperature as 540 degrees Rankine, the frequency as 3500 cycles per second, and the distance as .156 feet are assigned to K, C, and D, then $K = 4.525 \times 10^6$; $C = .196 \times 10^6$; and $D = 1135$. These values for the initial temperature, the frequency, and the distance are taken from typical runs. Using a full scale deflection of 180° on the phase angle meter, the phase angle could be read to the closest two degrees with accuracy. Therefore the term $d\Delta\phi$ in Eq. (61) is taken as two degrees. In a typical run, a phase angle of 10.266 degrees was observed for a temperature change of 70°, the initial temperature being 540 degrees Rankine. Substituting these values in Eq. (61) dT_2 is 9.25°R, an error of about 3%. In actuality, this is probably higher than the actual error since the phase meter could be used, for most conditions, with a full scale deflection of 36° where the phase angles could be determined to the nearest quarter of a degree. In Fig. 12 it is seen that the actual error did fall within these limits.

CHAPTER IV

EXPERIMENTAL CALIBRATION IN

SUBSONIC WIND TUNNEL.— In the first part of this chapter it was demonstrated that the temperature of a quantity of air might be determined by observing the phase shift between transmitted and received sound impulses which have traveled across the medium or by observing the frequency of sound needed for zero phase shift at some fixed distance. In this section, these ideas are directly applied to the temperature measurement of the air-stream in a subsonic wind tunnel to see if method will work in a moving temperature field which is essentially uniform.

First to be considered is the problem of the addition of a sound wave to a moving flow field. When the wave is introduced into the flow field, the wave length of the wave, with respect to a fixed observer, is in general, changed. The interaction between the wave and the field must be investigated to determine if, for the present case, a Doppler shift occurs.

Consider two walls moving with twice the speed of sound past a stationary air mass. Fig.6 shows this condition.

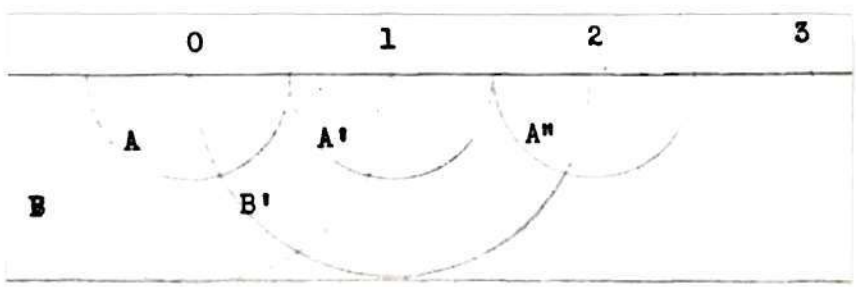

Figure 6
Sound Being Introduced **From Wall**

Although the situation pictured is supersonic, it may be generalized immediately to the subsonic case. In Fig. 6, the sound was originally radiated from position 0. When the sound is at A, the walls have moved to position 1 and have started to radiate a new wave. When the wave which originated from 0 is in position B, the walls are at 2 and the wave starting from 1 is at A'. As the walls reach position 3, the original wave is reaching C and the waves which started at 1 and 2 are at B' and A'' respectively. It is seen that the waves strike the walls perpendicularly at a distance downstream of twice the distance between the walls. Since the waves strike the walls perpendicularly, and since the distance between the walls is a constant, there will be no Doppler effect detectable to an observer moving with the walls.

If the air is moving and the walls stationary, there will be some question as to whether the waves will stay semi-spherical as they are moved downstream by the stream. A simple vector addition of the fields shows that this is the case. In some of the previously developed equations (Eq. (41), (47) and (48)) the distance between the transmitter and receiver is required. The distance which is used is the perpendicular distance between the transmitter and receiver, since at any instant each wave is still moving perpendicularly to the wall of the tunnel at the speed of sound.

A somewhat less intuitive approach may be followed. Young[15] derived the following equation when considering the matter of Doppler effect.

$$\frac{\nu}{\nu'} = \frac{1 - \left(\frac{l_o}{c_o} U_o + \frac{m_o}{c_o} V_o \right)}{1 - \left(\frac{l_i}{c_i} U_i + \frac{m_i}{c_i} V_i + \frac{n_i}{c_i} W_i \right)} \qquad (62)$$

where:

ν = original frequency
ν' = observed frequency
$U_o V_o W_o$ = velocity of sound source
U_1, V_1, W_1 = velocity of observer
$u\ v\ w$ = velocity of medium
$l\ m\ n$ = direction cosines of sound wave "rays"

This equation holds for the very general case of a moving observer, a moving sound source, and a moving medium. With this equation, the Doppler shift, $\frac{\nu}{\nu'}$, may be determined. In our case, the observer and the sound source are fixed. Therefore, U_o, V_o, U_1, W_o, W_1 are zero and $\nu/\nu' = 1$.

The sound generating and sound receiving apparatus is set up in the two dimensional jet in the nine foot wind tunnel at the Daniel Guggenheim School of Aeronautics. This is shown in Fig. 22. The method of finding the stream temperatures follow the frequency for zero phase shift method.

The purpose of this experiment was to see if the phase shift systems would work with air flowing between the phones. Since the Mach number in this experiment is so low, the temperature recovery factor is almost exactly 1.0 and a stagnation temperature thermometer will give an accurate measurement of the stream temperature. Therefore, to check the results of the phase shift method, the stream temperature was determined by stagnation temperature measurements and by using the equation

$$C_p T_o = C_p T_{STR} + \frac{V_{STR}^2}{2} \qquad (63)$$

The temperatures computed by this method were then compared with the temperatures measured by the phase shift method.

The stagnation temperature was measured by means of a stagnation thermometer placed in the stream which was observed through a plexiglas panel in the bottom of the tunnel. The velocity of the stream was determined by observing the pizeometer ring readings taken between the stagnation chamber and the test section. This difference in static pressures had previously been plotted as a function of true stream velocities.

It should be noted that at any instant during the experiment, the stream temperature was lower than the stagnation temperature, but as the experiment progressed, there was a stagnation temperature gradient, caused by friction heating of the tunnel walls and heat losses in the fan motor. Of course, this was accompanied by a free stream temperature gradient.

The experiment was performed in the following manner: the stagnation temperature was observed for a given tunnel velocity. At the same time, the frequency for zero phase angle was noted. The stream temperature as predicted by Bernoulli's equation and the stream temperature as determined by the phase method were plotted against tunnel velocity. Fig. 13 shows this result. The change in slope at the top of the graph is caused by the effect of the stagnation temperature gradient with time as previously mentioned.

It was found in the performance of this experiment that the high noise level of the tunnel at higher velocities introduced "hash" into the scope trace. Since the frequency for zero phase shift method was independent of the distance between the receivers, the phones were moved together. This effectively increased the signal-to-noise ratic to a point where the experiment became workable; i.e. the hash had been reduced to a point where the frequency for zero phase angle was determined accurately

by the trace on the oscilloscope. The distance used in the experiment was about one inch.

The results shown in Fig. 13 establish the fact that the phase shift method may be applied to the case of slowly moving air and very thin boundary layers for the measurement of temperature. The complexity of the method, however, when compared to the simplicity of a stagnation thermometer, would obviate any application of phase-shift temperature measurement in subsonic apparatus.

CHAPTER V

APPLICATION TO TEMPERATURE MEASUREMENT IN SUPERSONIC WIND TUNNEL

From the start of the experiment there was some doubt whether sound would ever traverse a supersonic stream. Therefore, the refracting effects of the velocity and temperature gradients in the boundary layer are investigated. The relationship between the speed of propagation in the medium, the velocity of the medium and the angle of refraction is, from optical considerations

$$\frac{a}{\sin\theta} + U = \text{Const.} \tag{64}$$

where:

a is the velocity of propagation

U is the velocity of the medium

θ is the angle between a ray and a perpendicular to the surface of discontinuity

This equation, developed by Lord Rayleigh[16], is applicable in the case of a moving medium and changing velocity of propagation when written between any two points in the field as shown in Eq.(65).

$$\frac{a_1}{\sin\theta_1} + U_1 = \frac{a_2}{\sin\theta_2} + U_2 \tag{65}$$

If point 1 is considered to be the wall, and point 2 the stream, the angle at the receiving wall may be solved for. The temperature in the stream may be found from the adiabatic relationship.

$$C_p T_o = C_p T + \frac{V^2}{2} \tag{66}$$

and the angle in the stream, θ_2, may be found by considering the figure below.

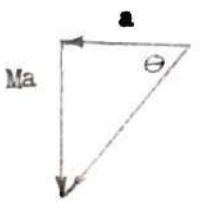

Figure 7
Angle of Ray in Stream

If the temperature of the air adjacent to the wall is considered to remain at the equilibrium stagnation temperature during the run, Eq. (65) may be solved for θ_1, the angle at the wall for different Mach numbers. These calculations are shown in Table 5 and are plotted in Fig. 14. This graph shows that there is no Mach number for which there is complete refraction in the second boundary layer.

The refraction in the second boundary layer may be investigated from another standpoint. Eq. (65) may be solved for the Mach number which gives a θ_1 of 90° at the wall.

$$a_1 = \frac{a_2}{\sin \theta_2} + U_2 \tag{67}$$

or

$$U_2 = a_1 - \frac{a_2}{\sin \theta_2} \tag{68}$$

and dividing by the speed of sound in the stream it is seen that

$$M_2 = \frac{a_1}{a_2} - \frac{1}{\sin \theta_2} \tag{69}$$

Considering Fig. 7, Eq. (69) may be rewritten.

$$M_2 = \sqrt{\frac{T_0}{T_2}} - \frac{\sqrt{M_2^2+1}}{M_2} = \sqrt{1+\frac{\gamma-1}{2}M_2^2} - \frac{\sqrt{M_2^2+1}}{M_2} \tag{70}$$

Now the only variable is the stream Mach number.

$$\left\{\left(\frac{\gamma+1}{2}\right)^2 - 2(\gamma-1)\right\} M_2^8 - 4M_2^6 - (\gamma+1)M_2^4 + 1 = 0 \tag{71}$$

Eq. (71) may be written

$$\left\{\left[\left(\frac{\gamma+1}{2}\right)^2 - 2(\gamma-1)\right]M_2^4 - 4M_2^2 - (\gamma+1)\right\} M_2^4 = 1 \tag{72}$$

from which it is seen that only imaginary solutions exist for M. This substantiates Fig. 14.

If no sound passes through the first boundary layer, it would be impossible to receive sound across the tunnel. If conditions at (1) are the wall and at (2) are the edge of the boundary layer Eq. (65) may be rewritten

$$\frac{a_1}{\rho \sin\theta_1} = a_2 + U_2 \tag{73}$$

since $U_1 = 0$, $\theta_2 = 90^\circ$, and simplying Eq. (73) it is seen that

$$\frac{\sqrt{\frac{T_1}{T_2}}}{\sin\theta_1} = 1 + M_2 \tag{74}$$

Substituting

$$\frac{T_0}{T_2} = 1 + \frac{\gamma-1}{2}M_2^2 \tag{75}$$

into Eq. (74), Eq. (76) is obtained.

$$\frac{\sqrt{1+.2M_2^2}}{\sin\theta_2} = 1+M_2 \tag{76}$$

The limiting case occurs when $\theta_1 = 90^o$. Under this condition, the sound leaves the source and is carried downstream in the boundary layer. Then solving Eq. (76) for the Mach number, it is found that

$$M_2 = 0, -2.5 \tag{77}$$

This theoretical work indicates that at least part of the sound propagated at right angles to a supersonic stream can traverse the stream regardless of the stream's Mach number.

An application of the phase shift method of measuring temperature was made to a Mach 2.0, 2" x 4" blowdown type supersonic wind tunnel. First, the frequency spectrum of the tunnel was analyzed. A General Radio Sound Level Meter and Frequency Analyzer were used in this analysis. The maximum sound intensity of the tunnel was found to be 132 decibels. This intensity was observed at 3500 cycles per second. A graph was plotted of the percent of this intensity occurring at frequencies throughout the spectrum and is shown in Fig. 15.

In both the frequency for zero phase shift method and direct phase angle observation method, it was necessary to know the temperature and frequency or phase angle at some arbitary condition. For this reason, three units were mounted on the tunnel. One unit was the sound transmitter, a fifty watt trumpet-type speaker-driver, and the other two units were magnetic earphones used as sound pickups. One receiving unit was mounted directly across the tunnel from the transmitter and was used to

find the initial conditions. The other earphone was mounted four inches downstream. This arrangement is shown in Fig. 8.

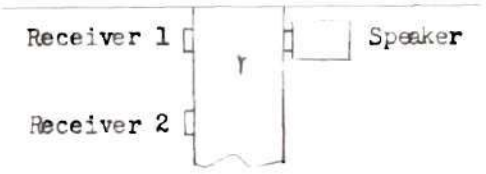

Figure 8
Mounting on Supersonic Tunnel

Fig. 23 shows the method of mounting the units in the tunnel's walls.

The second receiver was mounted downstream because as the sound traverses the stream it is carried downstream. Since the sound is being propagated with the velocity a, and the stream is moving with the velocity M.a (where M is the Mach number of the stream), it is seen that the receiver must be placed downstream a distance equal to the Mach number times the distance across the tunnel to intercept the sound. This is shown in the following equations.

$$\text{distance across tunnel} = a \times t \tag{78}$$

$$\text{distance downstream} = M \times a \times t \tag{79}$$

Therefore, Eq. (78) and (79) it is seen that

$$t = (\text{dist. across})/a = (\text{dist. downstr})/Ma \tag{80}$$

If distance downstream is solved for, Eq. (81) is obtained

$$\text{distance downstream} = M(\text{dist.across}) \tag{81}$$

The transmitting and receiving apparatus was installed in the

Mach two nozzle of a blowdown type supersonic wind tunnel. The nozzle was designed by William D.McCauley[17] for a Mach number of 2.05 and was found in previous tests to be within one half percent of this design value.

The frequency of sound used in this experiment was in the range of 500 cycles per second since the tunnel intensity at this frequency was relatively low and the efficiency of the earphone was good in this range. A bandpass filter with a sharp cut-off and high rejection was used to achieve an adequate signal-to-noise ratio. The filter used was a General Radio Sound Analyzer. This was the same unit which was used in the frequency spectrum determination.

The circuit used in the experiment is shown in Fig. 9.

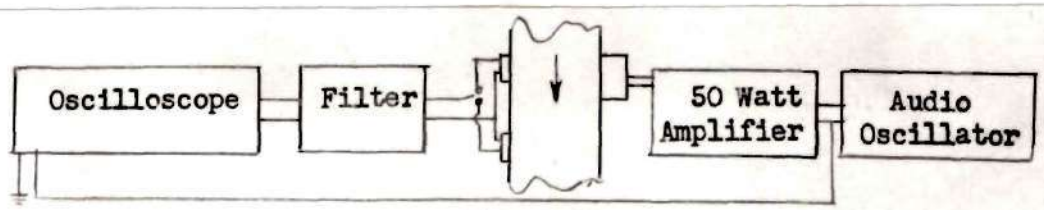

Figure 9
Circuit for Supersonic Experiment

The frequency for zero phase shift was noted with receiver 1 in the circuit, with the wind off. The stagnation temperature was noted also at this time. Because of the very sharp characteristics of the filter, at each frequency setting of the oscillator, the filter was readjusted until a peak was noted on the meter in the filter. Then the filter was passing the frequency which was being transmitted. The temperature of the stream was estimated by means of the adiabatic relationship and the frequency corresponding to this temperature and the initial temperature and frequency for zero phase shift was computed by Eq. (52). Using the

front receiver, the filter and oscillator were adjusted to this computed frequency with the wind off. The rear speaker was then switched into the circuit and the tunnel was run. The spacing on the trace of the scope was noted. The procedure was repeated for various , the spacing of the trace on the x 0 axis being noted each time.

The data are given in Table 5 and are plotted in Fig. 16. The plot is extrapolated to find the frequency for zero phase shift. The temperature predicted by the relationship

$$\frac{T_0}{T} = 1 + \frac{\gamma-1}{2} M^2 \tag{82}$$

is 298.3° for Mach number 2.0 and stagnation temperature of 537° Rankine. The temperature found by the frequency for zero phase shift method is 325° Rankine.

If the extrapolation of the graph in Fig. 16 is to have any significance, the general form of the equation connecting the spacing and the frequency must be obtained. The signal input to the x-axis may be written

$$x = k_1 \sin \omega t \tag{83}$$

and input to the y-axis may be written

$$y = k_2 \sin(\omega t + \phi) \tag{84}$$

The distance measured is actually the difference between the y coordinates at the two x 0 positions. Therefore at x = 0

$$\omega t = 0 \qquad y = k_2 \sin \phi \tag{85}$$

$$\omega t = \pi \qquad y = k_2 \sin(\phi + \pi) \tag{86}$$

and the spacing on the trace, $y_2 - y_1$, becomes

$$d = 2 k_2 \sin\phi \approx 2 k_2 \phi \tag{87}$$

Now the relationship between the frequency and the phase angle in successive runs must be linear since the number of waves between the speaker and receiver is a linear function of the frequency by Eq. (41). Therefore

$$\phi = k_3 \nu + k_4 \tag{88}$$

and

$$d \approx 2 k_2 (k_3 \nu + k_4) \tag{89}$$

This means that the spacing is a linear function of the frequency as zero phase shift is approached. To obtain the frequency for zero phase angle, the straight line faired through the three data points was extended until it intersected with the d 0 axis. The frequency obtained is 420cy and this corresponds to a temperature of 325° .

The probable error expected in the performance of this experiment is next computed. In this low range of frequencies the signal generator can be read to about 10 cycles per second. The general frequency for zero phase shift equation may be written

$$\sqrt{T_2} = \frac{\nu_2}{A} \tag{90}$$

where: $$A = \frac{\nu_1}{\sqrt{T_1}} = \text{const.}$$

and

$$\sqrt{T_2 + dT_2} = \frac{v_2 + dv_2}{A + dA} \tag{91}$$

where, as before in Eq. (56)

$$dA = \frac{dv}{\sqrt{T}} - \frac{1}{2}\frac{v}{T^{3/2}}dT = \frac{\pm 5}{\sqrt{537}} - \frac{1}{2}\frac{540}{537^{3/2}} = .238 \tag{92}$$

Therefore

$$dT_2 = \left(\frac{v_2 + dv_2}{A + dA}\right)^2 - T_2 = \left(\frac{420 \pm 5}{23.3 \pm .238}\right)^2 - 325 = \pm 13^\circ \tag{93}$$

A band of this width is plotted in Fig. 16 and it is seen that the experimental points fall within these limits.

The pressure differential on the diaphragm of the speaker is sufficient to reduce the output of the speaker to a point where the noise of the tunnel was overpowering and the speaker could not be heard across the tunnel without modification to the speaker. This situation was corrected by leading a pressure tap into the compartment behind the thin steel diaphragm. This is shown in Fig. 25.

Even with this pressure equalization, the diaphragm ruptured on two speaker units because of the high pressure pulses and high levels of output being used. Probably if larger diameter tubing had been used, the pressure equalization would have been rapid enough and the speaker would have withstood these extreme conditions.

CHAPTER VI

CONCLUSIONS

The performance of these experiments show that the temperature of subsonic and supersonic streams of air may be determined with a fair degree of accuracy by the electronic phase-shift methods described in this paper. The methods are not preferable in the subsonic case because conventional stagnation thermometers are accurate and very much more convenient. In the supersonic case, however, the phase-shift methods may well be worth the inconvenience. With the direct phase angle observation method applied in the supersonic case, a continuous and instantaneous record of the mean stream temperature can be obtained. This method is more preferable than a calibrated thermocouple since it is independent of the heating effects of the wall and may be used even while a model is being tested.

With some further development, the apparatus might be used in boundary layer measurement. The temperature measured is necessarily a mean temperature; i.e. including the temperature gradient in the boundary layer. With an approximate knowledge of the temperature profile and thickness, δ, the deflection of the zero streamline, might be investigated.

Several refinements suggested themselves during the performance of the experiments which might well be incorporated in future phase shift-temperature measurement experiments. In the direct phase angle measurement method, more damping would be helpful in the phase angle meter since rapid temperature fluctuations made the meter needle fluc-

tuate rapidly and a mean reading was sometimes difficult to obtain. This very quality, however, might be put to use by including in the circuit a continuous recording device which would show these fluctuations. In applying the methods to the temperature measurement of supersonic streams, a driving unit of sufficient durability should be used because the diaphragm is subjected to sharp pressure fluctuations.

BIBLIOGRAPHY

1. Kuethe, A. M. and Schetzer, J.D. Foundations of Aerodynamics. New York. John Wiley and Sons, 1950. p.303.

2. Pope, Alan Y. Aerodynamics of Supersonic Flight. New York. Pitman Publishing Corporation, 1950. p.11

3. Kuethe, op. cit., p.130.

4. Lamb, Horace. Hydrodynamics. 6th ed. Cambridge. University Press. p.646.

5. Tsien, Hsue-shin and Schamberg, Richard. Propagation of Plane Sound Waves in Rarefied Gases, Journal of the American Acoustical Society, 18 (Oct.1946)

6. Chapman and Cowling. Mathematical Theory of Non-Uniform Gases. Cambridge. University, 1939.

   Ibid. Heat transfer Measurements on Cones in the N.O.L. 40 x 40 cm. Supersonic Wind Tunnel No.2, White Oak, Md. Naval Ordinance Laboratory Publication NOLM 10106, 1950.

   Ibid. Determination of Temperature Recovery Factors on Cones in the N.O.L. 40 x 40 cm Supersonic Wind Tunnel No.2, White Oak, Md. Naval Ordinance Laboratory Publication NOLM 10107, 1950.

7. Wang Chang, C. S. and Ulenbeck, G. E. On the Transport Phenomena in Rarefied Gases. APL/JHU CM-443, Feb. 20, 1948.

8. Wang Chang, C. S. On Dispersion of Sound in Helium. APL/JHU CM-467, May 1, 1948.

9. Burnett, Proceedings of the Mathematical Society of London. 40 (1934).

10. Tisza, L. Supersonic Absorption and Stokes' Viscosity Relation, Physical Review, 61 (April, 1942). p.531.

11. Wang Chang, op. cit., p.2

12. Tisza, op. cit., p.533.

13. Tyzer, F. G. and Hardy, W. C. Properties of Felt in Reduction of Noise and Vibration, Journal of the Acoustical Society of America, 1947. p.872.

14. Goodman, I. Unpublished B.S. Thesis E.E. Department, Massachusetts Institute of Technology, 1943. Reprinted by Ernest Kretzner in Technology Instrument Corporation Instruction Manual for 320A Phase Meter. p.2.

15. Young, Robert E. The Doppler Effect for Sound in a Moving Medium, Journal of the Acoustical Society of America, 6 (Oct.1934) p.112.

16. Rayleigh, Lord. The theory of Sound. 2d ed. Cambridge. University Press. v.2. p.133.

APPENDIX

Table 1. Frequency for Zero Phase Shift Experimental Data.

Run A			Run B		
Temp.	ν	$\frac{\nu}{\sqrt{T}}$	Temp.	ν	$\frac{\nu}{\sqrt{T}}$
306	3810	217.8	304	3810	218.4
332	3875	212.6	335	3900	213.1
334	3900	213.3	339	3935	213.7
335	3915	213.9	342	3950	213.6
337	3925	213.7	346	3970	213.4
338	3935	214.1	350	4000	213.8
340	3950	214.2	356	4100	217.2
342	3960	214.1			
344	3978	214.4			
346	3990	214.5			
350	4003	213.9			
355	4110	218.1			

Table 2. Predicted Phase Shift for Various Initial Temperatures

	$T_1 = 539.6$			$T_1 = 549.6$			$T_1 = 559.6$	
T_2	$\frac{1}{\sqrt{T_2}}$	$\frac{1}{\sqrt{T_1}} - \frac{1}{\sqrt{T_2}}$	$\Delta\phi$	$\frac{1}{\sqrt{T_1}} - \frac{1}{\sqrt{T_2}}$	$\Delta\phi$	$\frac{1}{\sqrt{T_1}} - \frac{1}{\sqrt{T_2}}$	$\Delta\phi$
540	.04303	.00002	.0802	-.00037	-1.485	-.00076	-3.049
550	.04264	.00041	.1644	.00002	.0802	-.00037	-1.485
560	.04226	.00079	3.168	.00040	1.605	.00001	.0401
570	.04189	.00116	4.651	.00770	3.090	.00034	1.524
580	.04152	.00153	6.136	.00114	4.575	.00075	3.010
590	.04117	.00188	7.1539	.00149	5.979	.00110	4.414
600	.04082	.00223	8.943	.00184	7.383	.00145	5.818
610	.04049	.00256	10.266	.00217	8.708	.00178	7.143

$$\Delta\phi = \frac{360(.156)\ (3500)}{1.4 \times 1716} \left\{ \frac{1}{\sqrt{T_1}} - \frac{1}{\sqrt{T_2}} \right\}$$

$$= 4010.28 \left\{ \frac{1}{\sqrt{T_1}} - \frac{1}{\sqrt{T_2}} \right\}$$

Table 3. Observed Phase Shift for Various Initial Temperatures.

Run 1			Run 2		
$T^{o}R$	ϕ	$\Delta\phi$	T	ϕ	$\Delta\phi$
560	34.0	0	550	56.0	0
572	32.5	1.5	560	54.5	1.5
583	30.5	3.5	572	52.5	3.5
591	29.5	4.5	581	51.5	4.5
597	28.5	5.5	591	49.5	6.5
608	27.5	6.5	597	49.0	7
617	26.0	8.0	608	47.5	8.5
628	24.0	10.0	617	46.5	9.5
633	23.5	10.5			

Table 4. Subsonic Wind Tunnel Data.

			Stag.Pred.		ϕ Pred.
v	$v^2/12000$	T_0	T_2	v_2	T_2
0	0	549			
88	.645	550	549.35	3500	552.1
102.5	.866	553	552.13	3505	553.4
117.5	1.15	556	554.85	3510	552.1
127.1	1.35	560.5	559.15	3517	556.7
125	1.30	562.2	560.9	3530	561.1

$$v_1 = 3490$$
$$T_1 = 549$$
$$T_2 = T_1 (v_c / v_1)^2$$

Table 5. Angle at Wall Due to Refraction in Boundary Layer.

M	T_2	a_2	$\sin\theta_2$	$\frac{T_o}{T_2}$	$\frac{1}{\sin\theta_2}$	$\sqrt{\frac{T_o}{T_2}}$	$\frac{1}{\sin\theta_2}+M_2$	$\sin\theta_w$
.3	491.15	1086.21	.287	1.018	3.484	1.009	3.784	.2664
.6	466.41	1058.8	.514	1.072	1.945	1.035	2.545	.4067
.8	443.0	1020.3	.625	1.129	1.600	1.062	2.400	.4425
1	416.0	1000	.705	1.202	1.418	1.096	2.418	.4533
1.2	388.1	965.7	.768	1.288	1.302	1.135	2.502	.4534
1.3	373.7	947.5	.792	1.338	1.262	1.157	2.562	.4516
3	178.6	654.9	.948	2.799	1.054	1.673	4.054	.4127
2	277.7	817.1	.894	1.800	1.118	1.342	3.054	.4394
5	83	446	.981	6.024	1.0193	2.454	7.454	.3292
.1	499	1095.02	.099	1.002	10.101	1.001	10.201	.0981

M	θ_w	θ_s
.3	15.4	16.68
.6	24.0	30.93
.8	26.3	38.7
1	26.9	44.8
1.2	26.9	49.2
1.3	26.8	51.4
3	24.4	71.4
2	26.1	63.4
5	19.4	78.8
.1	5.6	5.7

$$T_2 = \frac{T_o}{1 + \frac{\gamma-1}{2} M^2}$$

$$a_2 = 49.02\sqrt{T_2}$$

$$\theta_s = \sin^{-1} M/\sqrt{M^2+1}$$

$$\theta_w = \sin^{-1} \frac{\sqrt{\frac{T_o}{T_2}}}{\frac{1}{\sin\theta_2} + M_2}$$

Table 6. Supersonic Wind Tunnel Phase Shift.

$T_t = 537$
$\phi_o = 540$

v	dist.
400	3
380	5
410	10

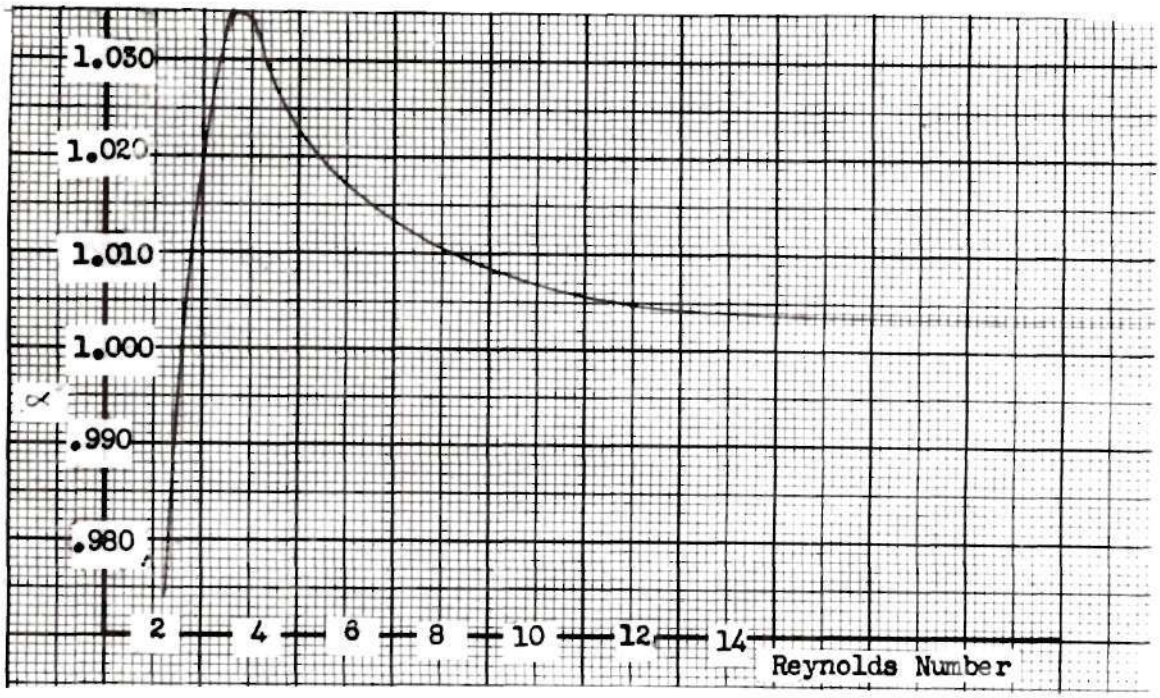

Figure 10
Reynolds Number versus ∝

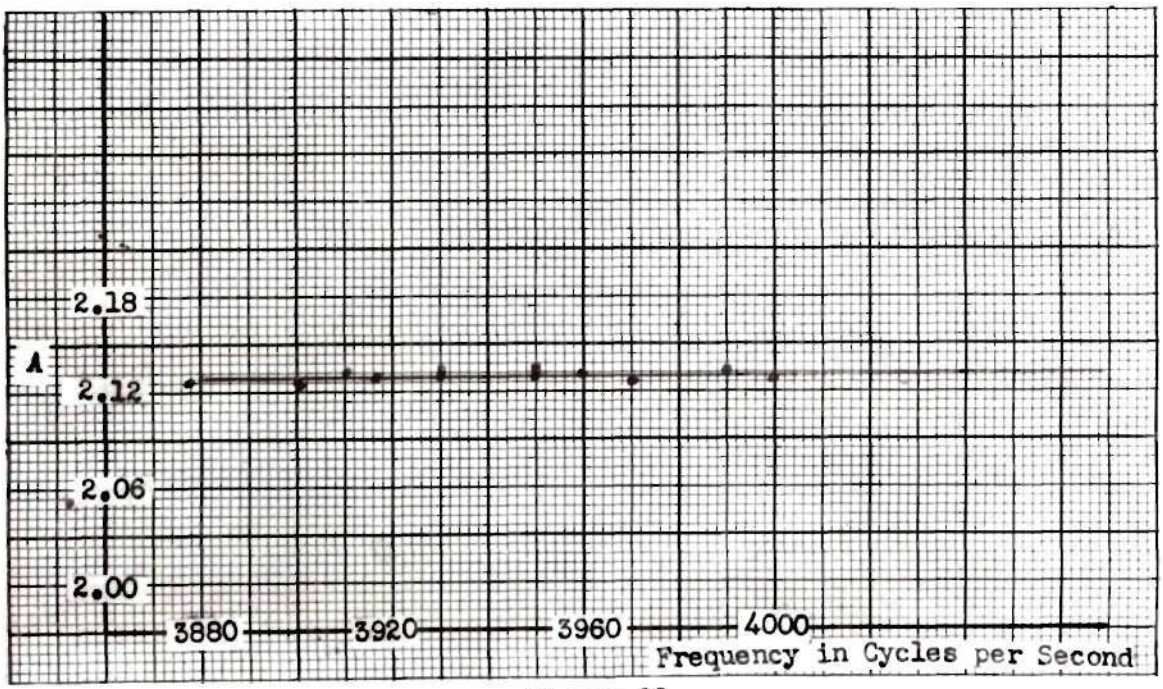

Figure 11
Frequency versus A

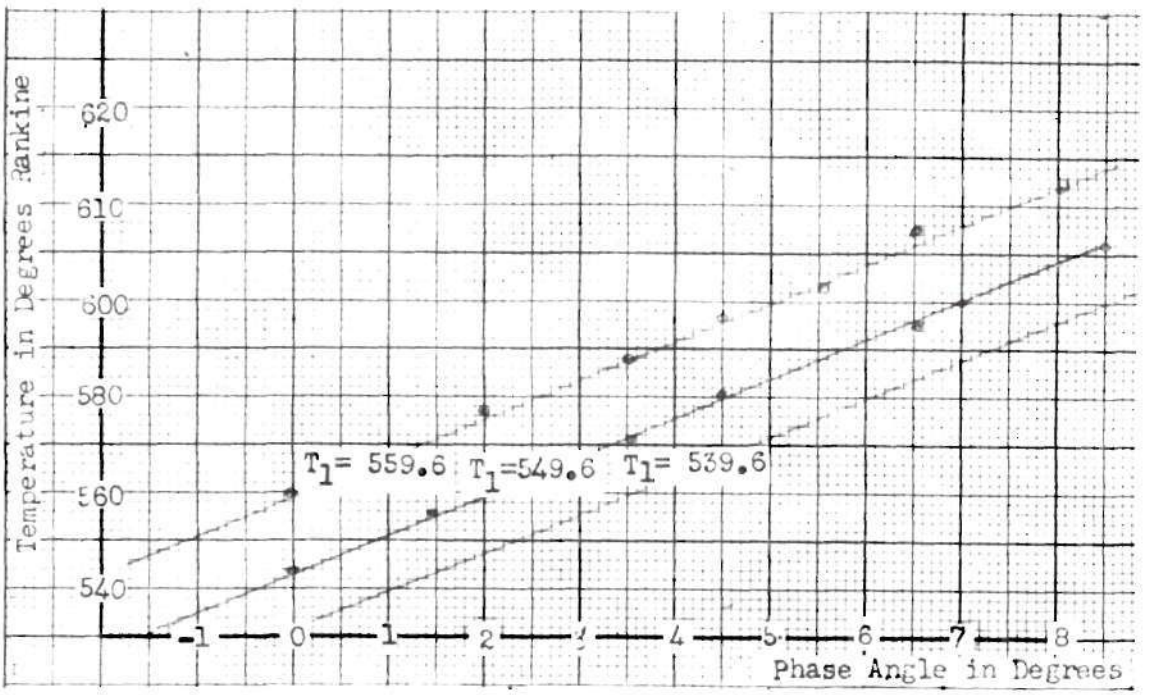

Figure 12
Predicted Temperatures For Observed Phase Angles

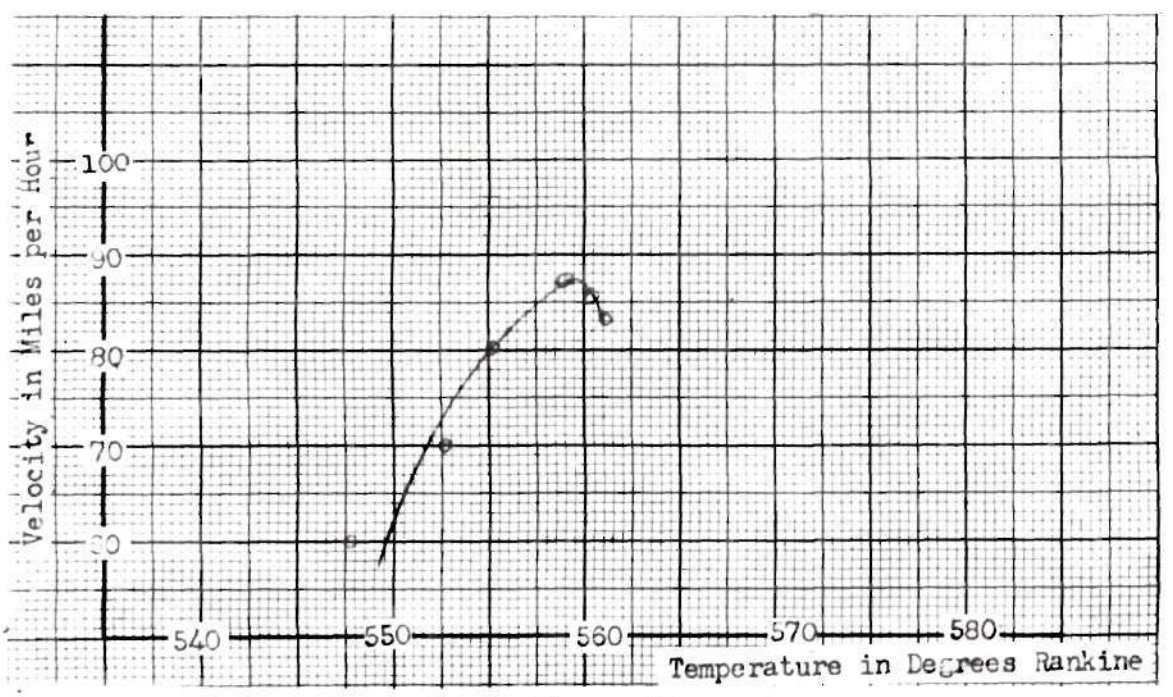

Figure 13
Subsonic Application

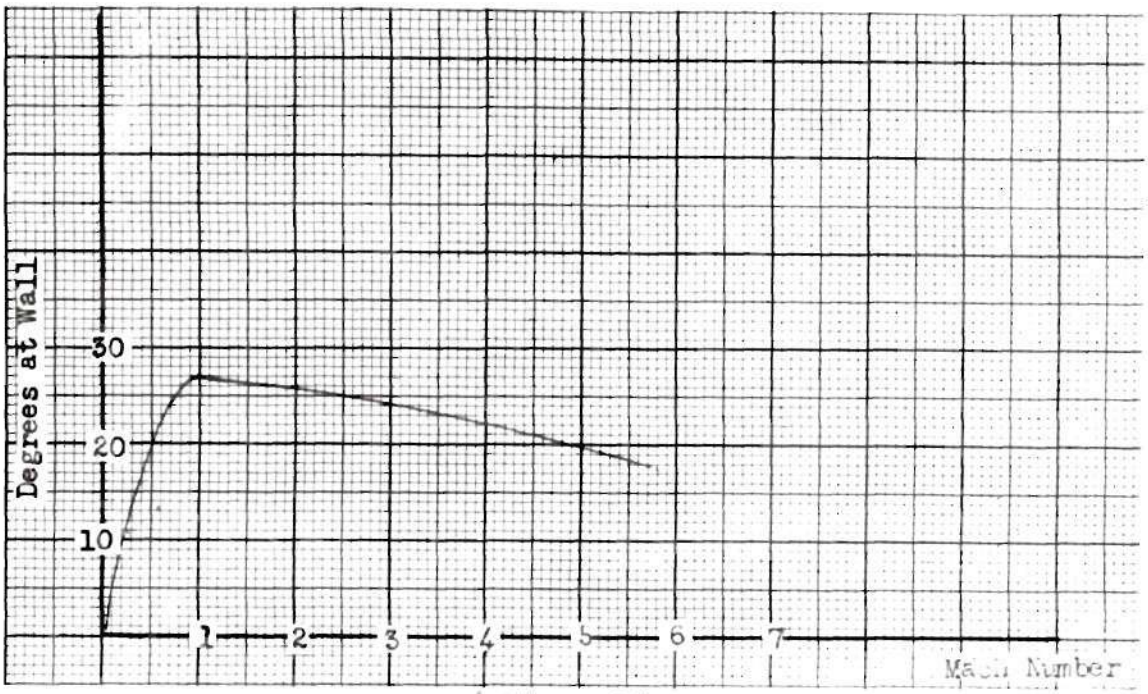

Figure 14
Sound Angle at Receiving Wall

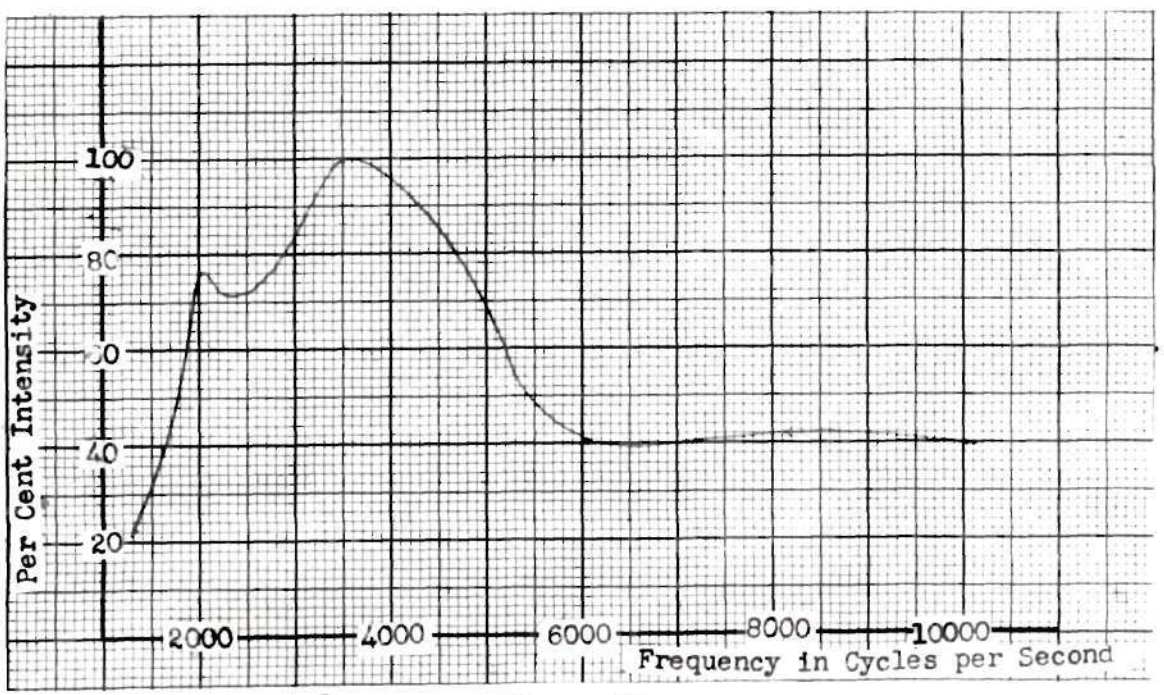

Figure 15
Sound Spectrum of Supersonic Tunnel

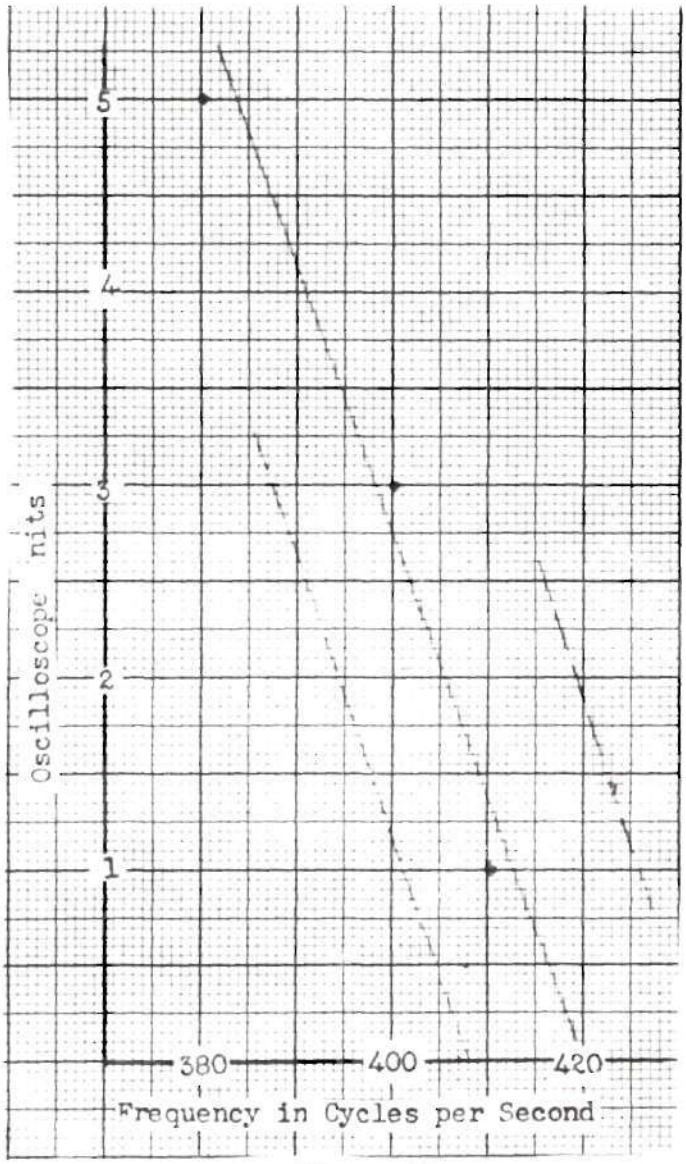

Figure 16
Supersonic Application

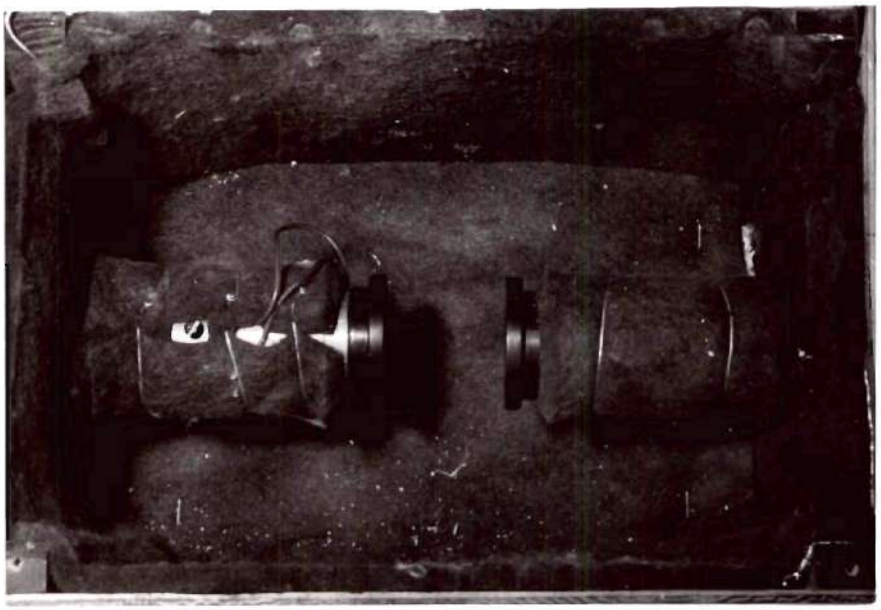

Figure 17
Box and Earphone Mountings

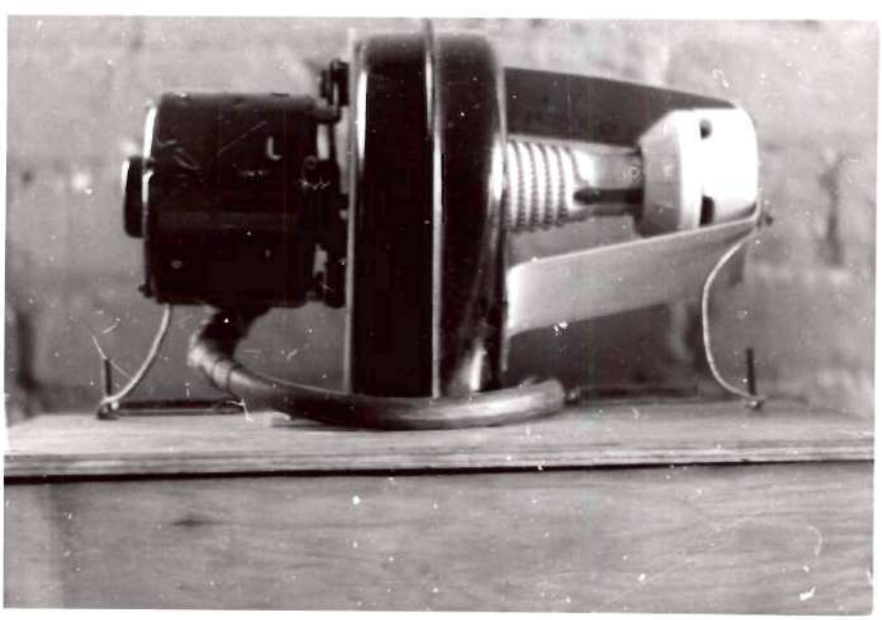

Figure 18
Blower

Figure 19
Oscilloscope Trace In-Phase

Figure 20
Oscilloscope Trace Out-of-Phase

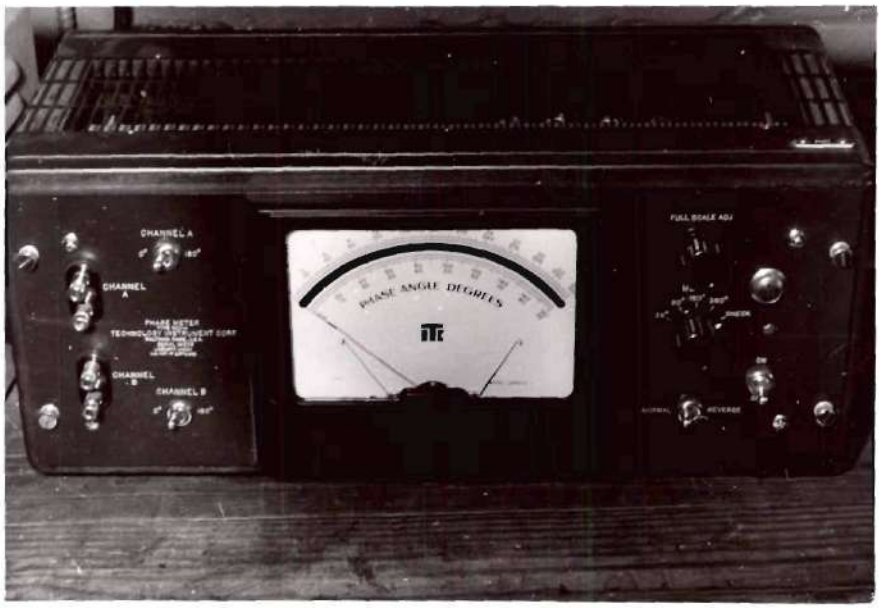

Figure 21
Phase Angle Meter

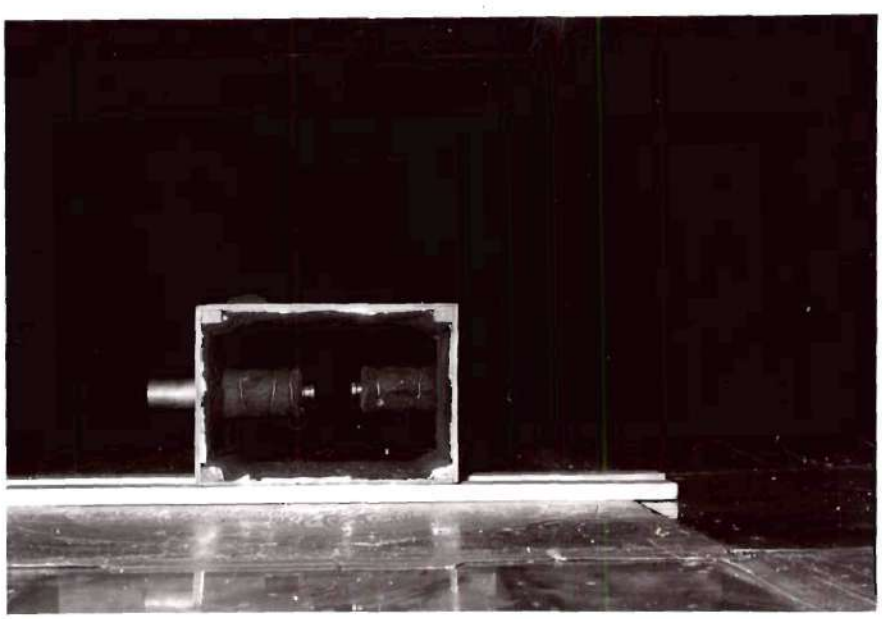

Figure 22
Subsonic Wind Tunnel Installation

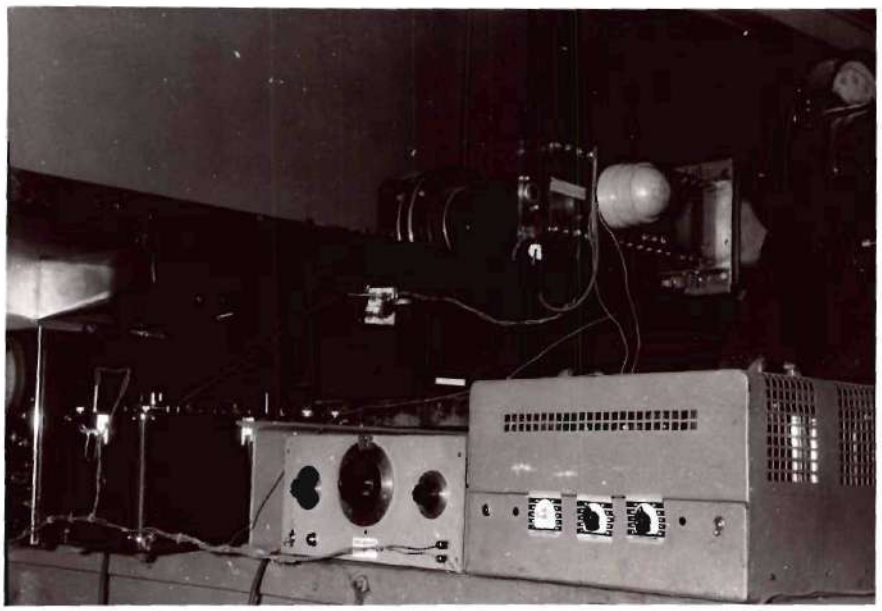

Figure 23
Installation in Supersonic Tunnel

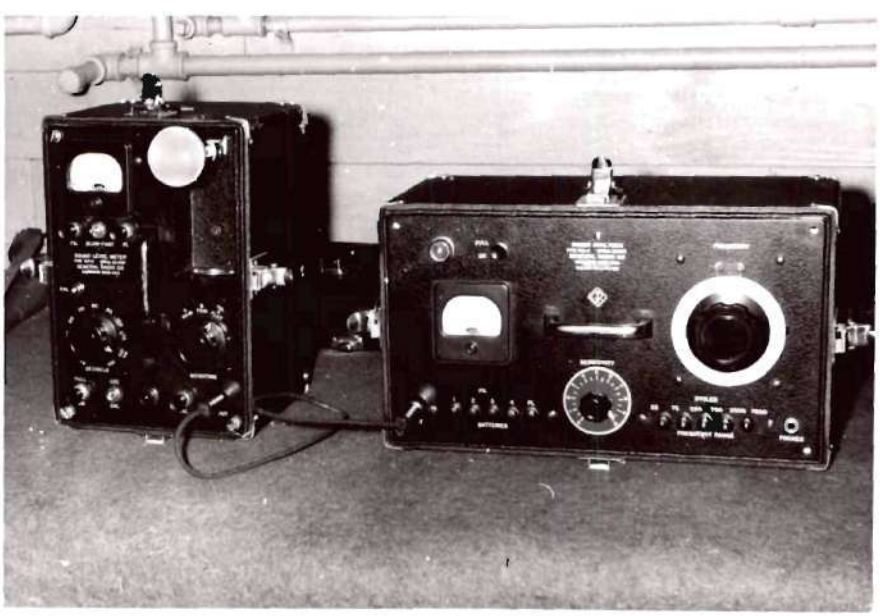

Figure 24
Frequency Measuring Equipment